0 9950-586

THE UNIVERSITY OF KANSAS CENTER FOR RESEA... INC.

2291 Irving Hill Drive—Campus West
Lawrence, Kansas 66045

Telephone: (913)864-4832

E83-10177
CR-169784

Adaptive Filtering of Radar Images for Autofocus Applications

(E83-10177) ADAPTIVE FILTERING OF RADAR IMAGES FOR AUTOFOCUS APPLICATIONS Final Report (Kansas Univ. Center for Research, Inc.) 39 p HC A03/MF A01 CSCL 17I

N83-17940

Unclas
G3/43 00177

J. A. Stiles
V. S. Frost
J. S. Gardner
D. R. Eland
K. S. Shanmugam
J. C. Holtzman

Remote Sensing Laboratory
Technical Report

RSL TR 489-1, Final Report

June 1981

Remote Sensing Laboratory
University of Kansas Center for Research, Inc.
Lawrence, Kansas 66045

ORIGINAL PAGE IS
OF POOR QUALITY

Supported by:

Jet Propulsion Laboratory
California Institute of Technology
under Contract 955 851

ABSTRACT

Autofocus techniques are being designed at the Jet Propulsion Laboratory to automatically choose the filter parameters (i.e., the focus) for the digital synthetic aperture radar correlator; currently, processing relies upon interaction with a human operator who uses his subjective assessment of the quality of the processed SAR data. Algorithms have been devised applying image cross-correlation to aid in the choice of filter parameters, but this method also has its drawbacks in that the cross-correlation result may not be readily interpretable. Enhanced performance of the cross-correlation techniques of JPL was hypothesized given that the images to be cross-correlated were first filtered to improve the signal-to-noise ratio for the pair of scenes. The results of experiments are described and images are shown.

LIST OF FIGURES

		Page
Figure 1	Multiplicative noise model for radar signals followed by cross-correlation, and then by minimum square error filtering as a preprocessing step for cross-correlation	9
Figure 2	Fading scenes (Images 1 and 2) were generated from a squared, segmented, averaged (within field boundaries) Seasat-A SAR image. White noise with a χ^2_2 probability density function was used in a multiplicative arrangement to produce fading scenes from the nonfading scene	10
Figure 3	Cross-correlation surface generation	11
Figure 4	Image 3 was computed from Image 1 using the adaptive filtering parameters "A" of Table 3. Image 4 was calculated from Image 2, also based upon parameters "A" of Table 3	12
Figure 5	Image 5 was generated from Image 1 using the adaptive filtering parameters "B" of Table 3. Image 6 was computed from Image 2, also based upon parameters "B" of Table 3	13
Figure 6	Shown above is the cross-correlation surface for Images 1 and 2 as photographed from an isometric display. The small trench running across the scene in the foreground of the peak is a display artifact. The peak has a generally pyramidal shape	14
Figure 7	Pictured above is the cross-correlation surface for Images 3 and 4. Cresting of the surface is seen; the shape is still primarily pyramidal	15
Figure 8	Illustrated above is the cross-correlation surface for Images 5 and 6. It has the same general characteristics as seen in Figure 7	16
Figure 9	The three cross-correlation peaks shown from above	17
Figure 10	The three correlation peaks identically scaled, from a side view. The center peak belongs to the cross-correlation of Images 1 and 2 and has a lower intensity	18
Figure 11	Side view of cross-correlation surface of Images 1 and 2. Identical scales were used for photographs on this page	19

LIST OF TABLES

Page

Table 1 Cross-Correlation Inputs 20

Table 2 Filter Parameters and Their Functions 21

Table 3 Filter Parameters Applied to Fading Scenes 22

Table 4 Cross-Correlation Results 23

Table 5 Width of the Correlation Surface Peak at Several Intensity Levels Below the Maxima (8 bit quantization of cross-correlation functions, all scaled identically by an arbitrary constant) 24

1.0 INTRODUCTION

The Jet Propulsion Laboratory maintains a digital synthetic aperture radar correlator which is now being utilized to process the raw data from the Seasat-A SAR mission which took place in 1978. The data represent the complex video signal, and they must be filtered to produce images suitable for viewing. Currently, filter parameters are chosen by a human operator, based solely upon subjective evaluation of image "quality". Alternative means for determining the "focus" parameters have been sought by JPL. One technique consists of cross-correlating images generated as, say, the first and fourth looks which originate from distinct spectral components of the complex SAR images.

As discussed in JPL internal memoranda [1, 2], when the SAR data are not optimally focused, the first and fourth look images will be offset from each other spatially, and the offset can, theoretically, be determined through registration techniques (using cross-correlation algorithms). However, the images generated have statistically independent noise degradation (i.e., independent fading noise) since the scenes arise from different portions of the complex spectrum of the SAR data. Although the underlying microwave reflectivity scene is ideally the same for the image being correlated, a strong correlation peak cannot usually result due to the formation of different noise sample functions in the two scenes.

It was proposed that the cross-correlation approach would work better if the two scenes were first filtered to improve signal-to-noise characteristics, prior to cross-correlating. An adaptive minimum mean square error image filter developed by Frost et al. [3] at the Remote Sensing Laboratory was candidate for preprocessing two one-look images "amplitude" image was squared so that intensities could be displayed. Next, the image was segmented into "homogeneous" regions as determined by field boundaries (the scene is an agriculturally developed region in Iowa).

The noisy areas within the field boundaries were "colored over" on the digital image display at the Remote Sensing Laboratory, with the mean values of those areas determining the intensity that would replace the fading scene. Next, this segmented, averaged image (shown in Figure 2) was input to an algorithm which regenerates fading values according to the relation [5, 6]

$$P_R = \frac{\overline{P_R}}{2N} \cdot y \qquad (1)$$

where N represents the number of looks for the radar (assumed integer) and y is a random variable whose probability density function is given as a χ^2_{2N}. Thus, a random number generator was employed to replace average intensities. No pixel correlation was used to color the spectrum of the noise; this approach is supported by the observation that the pixel-to-pixel correlation is not highly significant for N = 1 images even though there are several pixels per resolution distance (actual experiments were conducted with the SAR 580 N = 1 data, which was digitally processed, and not sampled at the large interval (~ 17 m) of the commercially available Seasat-A SAR data). Since white noise was used, it is possible the results of the overall experiment would change somewhat if samples were correlated (say, run through a linear filter prior to multiplication with the "defaded" scene).

Two N = 1 images were computer generated with different noise sample functions as seen in Figure 2. These images were next input

.0 CORRELATION RESULTS

The cross-correlation surface peak and its surrounding region for Images 1 and 2 is shown in Figure 6. It is characterized by a weak correlation maximum, and it is pyramidal in shape, with no strong side-lobe structure. This surface was photographed from an isometric display; a 64 by 64 pixel region from the original 512 by 512 pixel surface is represented. The equivalent rectangular width of this surface is 53 pixels by 53 pixels. The peak value of the cross-correlation is listed in Table 4. The cross-correlation of Images 3 and 4 is viewed in Figure 7. The adaptive filtering effects have caused the cross-correlation peak to have more sharply crested zones away from the peak. The equivalent rectangular width is 57 pixels square; the cross-correlation peak is listed in Table 4. Likewise, the cross-correlation of Images 5 and 6 (processed with identical filter parameters (B) of Table 4) is shown in Figure 8. Again, it is noted that a more sharply crested fall-off of the peak is produced by the MMSE filtering. The equivalent rectangular width is 59 pixels square; the cross-correlation peak is listed in Table 4.

The three cross-correlations are shown together in Figures 9 and 10. Note that all images were scaled identically so that a direct comparison could be made. To examine more closely the fine structure of the peaks, they were rephotographed as side views, and they are shown in Figures 11, 12, and 13. We see that although the cross-correlation of Images 1 and 2 (original fading images), which is given as Figure 11, has a smaller equivalent rectangular width than the preprocessed cross-correlations, it is apparent that the surface is sharper near the peak for Figures 12 and 13 (Image 3 cross-correestimator and research is continuing along these lines.

Previous research of Fries and Modestino [8] has shown the statistical limitation of the autocorrelation peak for scenes similar to the "source" image of Figure 2. Thus, it is known that the cross-correlation peak cannot rise above a certain level on the average, even if the two image inputs to the cross-correlation consisted of identical values $\hat{r}(t)$ on a pixel-by-pixel basis due to preprocessing. That is, the type of scene limits its own unnormalized autocorrelation peak. Fries and Modestino also have shown this effect to be functionally dependent on edge density and average intensity correlation between neighboring fields [8]. One could consider the agricultural test region chosen to be somewhat a worst case example of SAR scenes for analysis. The greatest difference in cross-correlation peaks for nonprocessed versus preprocessed scenes would be seen for two independent, white noise fields; this case might be thought of as the best case for demonstrating potential of the MMSE filtering approach.

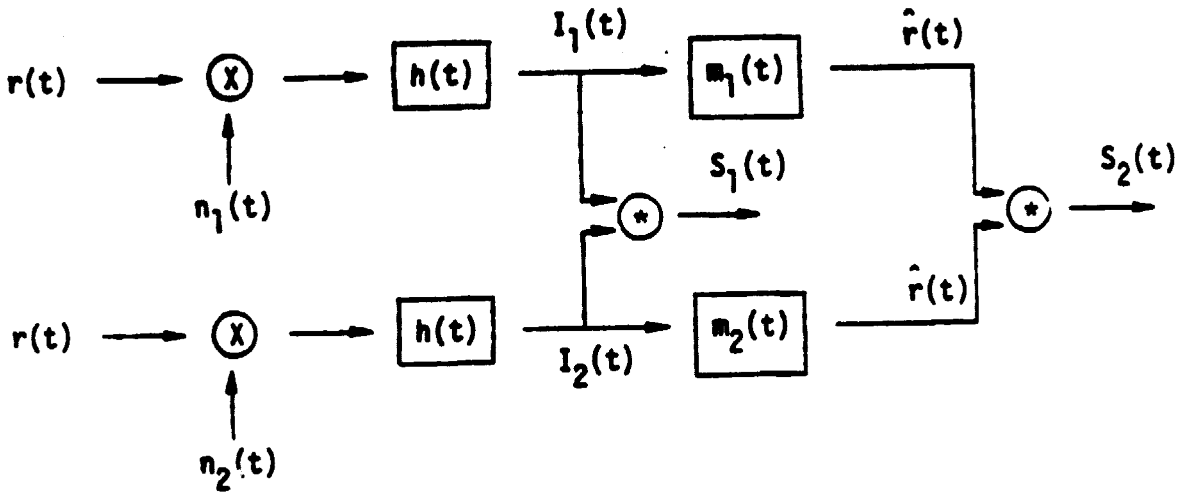

Figure 1. Multiplicative noise model for radar signals followed by cross-correlation, and then by minimum mean square error filtering as a preprocessing step for cross-correlation.

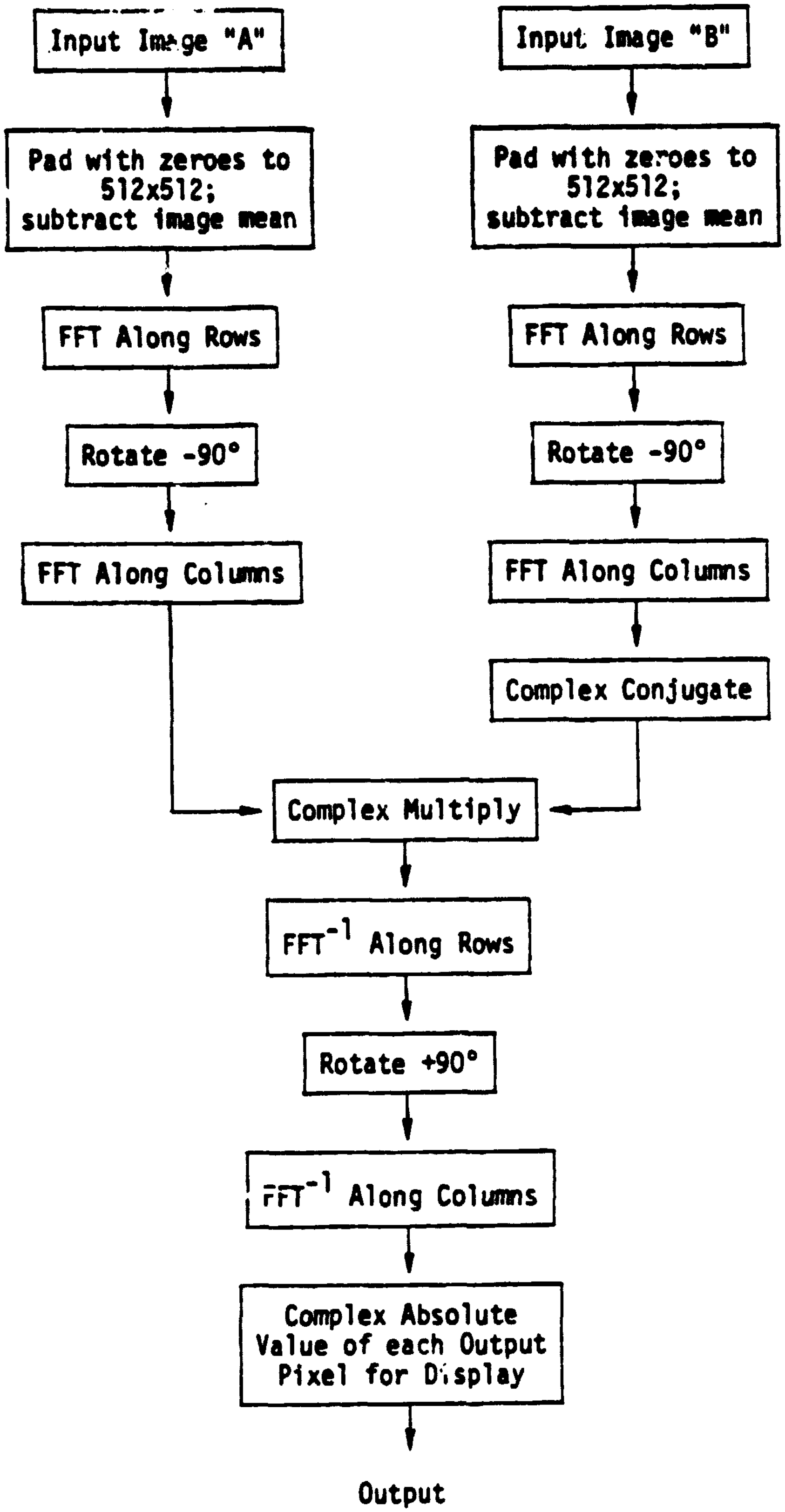

Figure 3. Cross-correlation surface generation.

ORIGINAL PAGE IS
OF POOR QUALITY

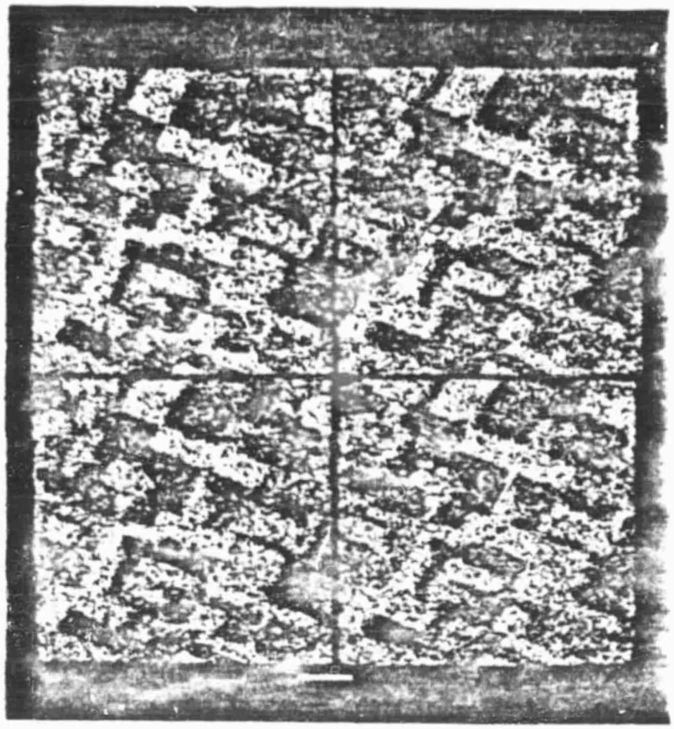

Figure 5. Image 5 was generated from Image 1 using the adaptive filtering parameters "B" of Table 3. Image 6 was computed from Image 2, also based upon parameters "B" of Table 3.

PRECEDING PAGE BLANK NOT FILMED

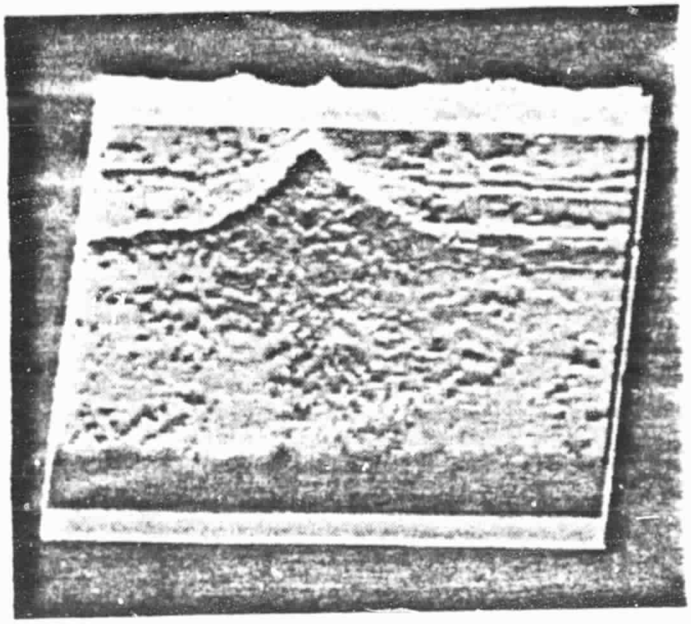

Figure 7. Pictured above is the cross-correlation surface for Images 3 and 4. Cresting of the surface is seen; the shape is still primarily pyramidal.

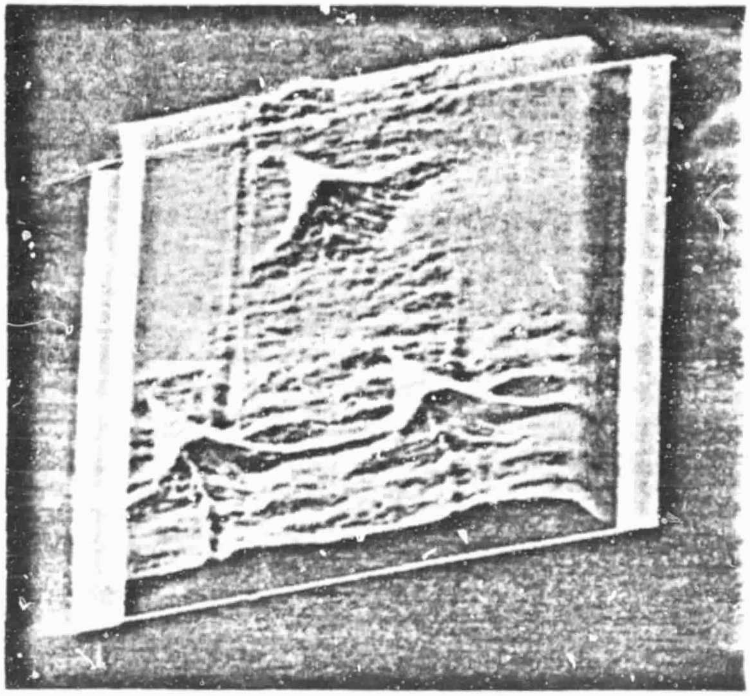

Figure 9. The three cross-correlation peaks shown from above.

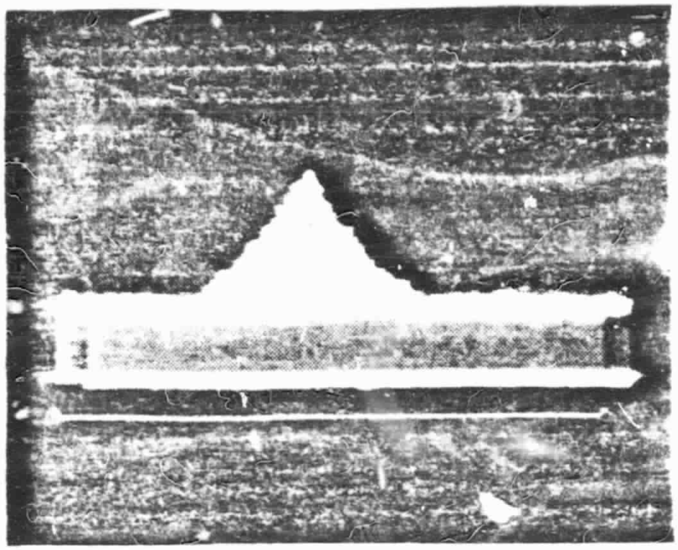

Figure 11. Side view of cross-correlation surface of Images 1 and 2. Identical scales were used for photographs on this page.

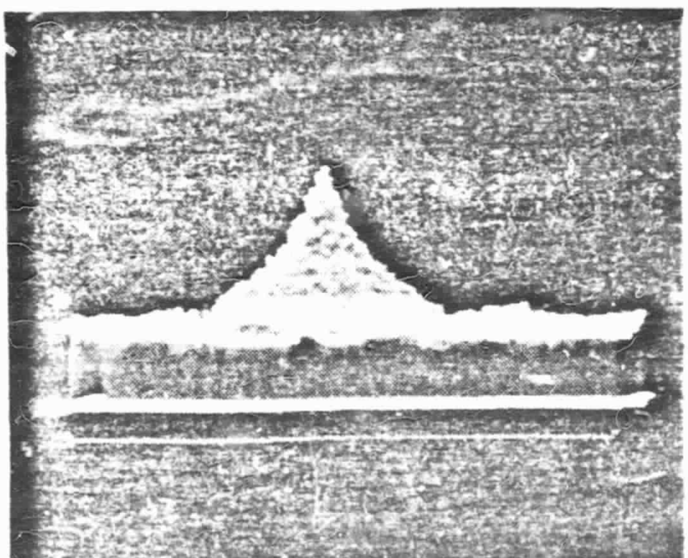

Figure 12. Side view of cross-correlation surface of Images 3 and 4.

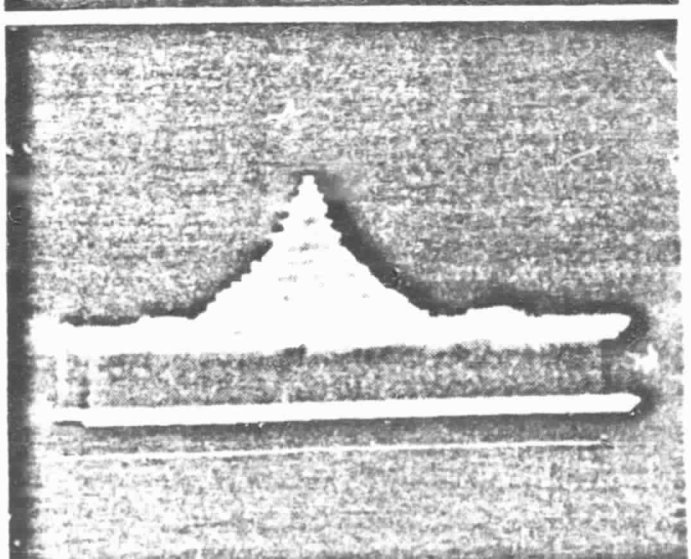

Figure 13. Side view of cross-correlation surface of Images 5 and 6.

Table 2

Filter Parameters and Their Functions

Parameters	Functions
Filter Size	filter impulse response width
Number of Filters (NF)	sets NF-1 thresholds for σ^2/μ^2, which are then mapped into filter indices
Observation Window Size	window size in which σ^2 and μ^2 are computed
Maximum Alpha	sets the rate of decay within a filter as a function of filter index
Input Gain	multiplying factor on the input pixel values
Alpha Bias	adjusts the filter indices up or down
Alpha Gain	maps the observed noise-to-signal ratio (σ^2/μ^2) into a filter index

Table 4

Cross-Correlation Results

Image Number	Correlation Peak ($\times 10^7$)	Equivalent Rectangular Width
1 and 4	1.648	53.0
2 and 5	2.096	58.7
3 and 6	2.020	58.4
7 (autocorrelation)	1.986	----

APPENDIX

The minimum mean square error filter for stochastic estimation of fading radar signals based upon the multiplicative SAR image model [5, 6] was developed and reported previously [7, 3]. The implementation of this filter, in effect, determines whether a region under observation is "homogeneous" (e.g., a white noise field) or not (contains a boundary, or for some other reason possesses a signal-to-noise ratio lower than the theoretically calculable value). NF-1 thresholds exist with which to compare the observed value of σ^2/μ^2, where

$$\mu = \frac{1}{(ws)^2} \sum_{i=1}^{(ws)^2} x_i$$

$$\sigma^2 = \frac{1}{(ws)^2-1} \sum_{i=1}^{(ws)^2} (x_i - \mu)^2$$

ws equals the window dimension (square in this implementation).

The quantized levels of σ^2/μ^2 are mapped into filter indices, NF total filters. The filter chosen is used as a mask to multiply on a pixel-by-pixel basis with the underlying image data. As the observation window moves, different filters are picked to apply to the data. Within a filter, the exponential decay of weightings is governed by the constant alpha max.

The following computer output lists the filters used on Image 3 (generated from Image 1) and gives the number of filter usages.

The adaptive implementation of the MMSE filter was written by Stephan A. Smith* and Victor Frost of the Remote Sensing Laboratory.

*Now at Texas Instruments, Dallas, Texas.

SNUMB = 1473T, ACTIVITY # = 04, , REPORT CODE = 52, RECORD COUNT = 000488

THIS IS FILTER # 1

0.020408	0.020408	0.020408	0.020408	0.020408	0.020408	0.020408
0.020408	0.020408	0.020408	0.020408	0.020408	0.020408	0.020408
0.020408	0.020408	0.020408	0.020408	0.020408	0.020408	0.020408
0.020408	0.020408	0.020408	0.020408	0.020408	0.020408	0.020408
0.020408	0.020408	0.020408	0.020408	0.020408	0.020408	0.020408
0.020408	0.020408	0.020408	0.020408	0.020408	0.020408	0.020408
0.020408	0.020408	0.020408	0.020408	0.020408	0.020408	0.020408

THIS IS FILTER # 2

0.016415	0.017850	0.018922	0.019331	0.018922	0.017850	0.016415
0.017850	0.019772	0.021375	0.022049	0.021375	0.019772	0.017850
0.018922	0.021375	0.023816	0.025150	0.023816	0.021375	0.018922
0.019331	0.022049	0.025150	0.028687	0.025150	0.022049	0.019331
0.018922	0.021375	0.023816	0.025150	0.023816	0.021375	0.018922
0.017850	0.019772	0.021375	0.022049	0.021375	0.019772	0.017850
0.016415	0.017850	0.018922	0.019331	0.018922	0.017850	0.016415

THIS IS FILTER # 3

0.012972	0.015340	0.017238	0.017990	0.017238	0.015340	0.012972
0.015340	0.018821	0.021996	0.023406	0.021996	0.018821	0.015340
0.017238	0.021996	0.027307	0.030452	0.027307	0.021996	0.017238
0.017990	0.023406	0.030452	0.039618	0.030452	0.023406	0.017990
0.017238	0.021996	0.027307	0.030452	0.027307	0.021996	0.017238
0.015340	0.018821	0.021996	0.023406	0.021996	0.018821	0.015340
0.012972	0.015340	0.017238	0.017990	0.017238	0.015340	0.012972

THIS IS FILTER # 4

0.010064	0.012942	0.015416	0.016436	0.015416	0.012942	0.010064
0.012942	0.017588	0.022221	0.024391	0.022221	0.017588	0.012942
0.015416	0.022221	0.030737	0.036197	0.030737	0.022221	0.015416
0.016436	0.024391	0.036197	0.053715	0.036197	0.024391	0.016436
0.015416	0.022221	0.030737	0.036197	0.030737	0.022221	0.015416
0.012942	0.017588	0.022221	0.024391	0.022221	0.017588	0.012942
0.010064	0.012942	0.015416	0.016436	0.015416	0.012942	0.010064

THIS IS FILTER # 5

0.007660	0.010712	0.013527	0.014733	0.013527	0.010712	0.007660
0.010712	0.016125	0.022024	0.024938	0.022024	0.016125	0.010712
0.013527	0.022024	0.033943	0.042212	0.033943	0.022024	0.013527
0.014733	0.024938	0.042212	0.071452	0.042212	0.024938	0.014733
0.013527	0.022024	0.033943	0.042212	0.033943	0.022024	0.013527
0.010712	0.016125	0.022024	0.024938	0.022024	0.016125	0.010712
0.007660	0.010712	0.013527	0.014733	0.013527	0.010712	0.007660

0.004116	0.013924	0.041057	0.070809	0.041057	0.013924	0.004116
0.002297	0.006386	0.013924	0.018995	0.013924	0.006386	0.002297
0.000993	0.002297	0.004116	0.005096	0.004116	0.002297	0.000993

THIS IS FILTER # 12

0.000663	0.001668	0.003169	0.004008	0.003169	0.001668	0.000663
0.001668	0.005138	0.012109	0.017041	0.012109	0.005138	0.001668
0.003169	0.012109	0.039784	0.072456	0.039784	0.012109	0.003169
0.004008	0.017041	0.072456	0.308076	0.072456	0.017041	0.004008
0.003169	0.012109	0.039784	0.072456	0.039784	0.012109	0.003169
0.001668	0.005138	0.012109	0.017041	0.012109	0.005138	0.001668
0.000663	0.001668	0.003169	0.004008	0.003169	0.001668	0.000663

THIS IS FILTER # 13

0.000436	0.001193	0.002402	0.003103	0.002402	0.001193	0.000436
0.001193	0.004068	0.010366	0.015049	0.010366	0.004068	0.001193
0.002402	0.010366	0.037948	0.072984	0.037948	0.010366	0.002402
0.003103	0.015049	0.072984	0.353962	0.072984	0.015049	0.003103
0.002402	0.010366	0.037948	0.072984	0.037948	0.010366	0.002402
0.001193	0.004068	0.010366	0.015049	0.010366	0.004068	0.001193
0.000436	0.001193	0.002402	0.003103	0.002402	0.001193	0.000436

THIS IS FILTER # 14

0.000283	0.000840	0.001794	0.002368	0.001794	0.000840	0.000283
0.000840	0.003175	0.008746	0.013097	0.008746	0.003175	0.000840
0.001794	0.008746	0.035672	0.072450	0.035672	0.008746	0.001794
0.002368	0.013097	0.072450	0.400784	0.072450	0.013097	0.002368
0.001794	0.008746	0.035672	0.072450	0.035672	0.008746	0.001794
0.000840	0.003175	0.008746	0.013097	0.008746	0.003175	0.000840
0.000283	0.000840	0.001794	0.002368	0.001794	0.000840	0.000283

THIS IS FILTER # 15

0.000181	0.000584	0.001322	0.001782	0.001322	0.000584	0.000181
0.000584	0.002445	0.007280	0.011246	0.007280	0.002445	0.000584
0.001322	0.007280	0.033084	0.070958	0.033084	0.007280	0.001322
0.001782	0.011246	0.070958	0.447731	0.070958	0.011246	0.001782
0.001322	0.007280	0.033084	0.070958	0.033084	0.007280	0.001322
0.000584	0.002445	0.007280	0.011246	0.007280	0.002445	0.000584
0.000181	0.000584	0.001322	0.001782	0.001322	0.000584	0.000181

THIS IS FILTER # 16

0.000114	0.000401	0.000962	0.001325	0.000962	0.000401	0.000114
0.000401	0.001859	0.005986	0.009538	0.005986	0.001859	0.000401
0.000962	0.005986	0.030308	0.068645	0.030308	0.005986	0.000962
0.001325	0.009538	0.068645	0.494050	0.068645	0.009538	0.001325
0.000962	0.005986	0.030308	0.068645	0.030308	0.005986	0.000962
0.000401	0.001859	0.005986	0.009538	0.005986	0.001859	0.000401
0.000114	0.000401	0.000962	0.001325	0.000962	0.000401	0.000114

0.000183	0.002907	0.046068	0.730174	0.046068	0.002907	0.000183
0.000117	0.001514	0.014667	0.046068	0.014667	0.001514	0.000117
0.000034	0.000295	0.001514	0.002907	0.001514	0.000295	0.000034
0.000006	0.000034	0.000117	0.000183	0.000117	0.000034	0.000006

THIS IS FILTER # 23

0.000004	0.000022	0.000080	0.000129	0.000080	0.000022	0.000004
0.000022	0.000211	0.001174	0.002326	0.001174	0.000211	0.000022
0.000080	0.001174	0.012677	0.042049	0.012677	0.001174	0.000080
0.000129	0.002326	0.042049	0.760199	0.042049	0.002326	0.000129
0.000080	0.001174	0.012677	0.042049	0.012677	0.001174	0.000080
0.000022	0.000211	0.001174	0.002326	0.001174	0.000211	0.000022
0.000004	0.000022	0.000080	0.000129	0.000080	0.000022	0.000004

THIS IS FILTER # 24

0.000002	0.000014	0.000055	0.000090	0.000055	0.000014	0.000002
0.000014	0.000151	0.000906	0.001852	0.000906	0.000151	0.000014
0.000055	0.000906	0.010902	0.038187	0.010902	0.000906	0.000055
0.000090	0.001852	0.038187	0.787459	0.038187	0.001852	0.000090
0.000055	0.000906	0.010902	0.038187	0.010902	0.000906	0.000055
0.000014	0.000151	0.000906	0.001852	0.000906	0.000151	0.000014
0.000002	0.000014	0.000055	0.000090	0.000055	0.000014	0.000002

THIS IS FILTER # 25

0.000001	0.000009	0.000037	0.000062	0.000037	0.000009	0.000001
0.000009	0.000107	0.000697	0.001468	0.000697	0.000107	0.000009
0.000037	0.000697	0.009334	0.034525	0.009334	0.000697	0.000037
0.000062	0.001468	0.034525	0.812065	0.034525	0.001468	0.000062
0.000037	0.000697	0.009334	0.034525	0.009334	0.000697	0.000037
0.000009	0.000107	0.000697	0.001468	0.000697	0.000107	0.000009
0.000001	0.000009	0.000037	0.000062	0.000037	0.000009	0.000001

THIS IS FILTER # 26

0.000001	0.000006	0.000025	0.000043	0.000025	0.000006	0.000001
0.000006	0.000076	0.000533	0.001159	0.000533	0.000076	0.000006
0.000025	0.000533	0.007960	0.031092	0.007960	0.000533	0.000025
0.000043	0.001159	0.031092	0.834162	0.031092	0.001159	0.000043
0.000025	0.000533	0.007960	0.031092	0.007960	0.000533	0.000025
0.000006	0.000076	0.000533	0.001159	0.000533	0.000076	0.000006
0.000001	0.000006	0.000025	0.000043	0.000025	0.000006	0.000001

THIS IS FILTER # 27

0.000000	0.000004	0.000017	0.000030	0.000017	0.000004	0.000000
0.000004	0.000054	0.000407	0.000912	0.000407	0.000054	0.000004
0.000017	0.000407	0.006765	0.027904	0.006765	0.000407	0.000017
0.000030	0.000912	0.027904	0.853920	0.027904	0.000912	0.000030
0.000017	0.000407	0.006765	0.027904	0.006765	0.000407	0.000017
0.000004	0.000054	0.000407	0.000912	0.000407	0.000054	0.000004
0.000000	0.000004	0.000017	0.000030	0.000017	0.000004	0.000000

0.000002	0.000076	0.002421	0.013851	0.002421	0.000076	0.000002
0.000003	0.000206	0.013851	0.933430	0.013851	0.000206	0.000003
0.000002	0.000076	0.002421	0.013851	0.002421	0.000076	0.000002
0.000000	0.000006	0.000076	0.000206	0.000076	0.000006	0.000000
0.000000	0.000000	0.000002	0.000003	0.000002	0.000000	0.000000

THIS IS FILTER # 34

0.000000	0.000000	0.000001	0.000002	0.000001	0.000000	0.000000
0.000000	0.000004	0.000057	0.000159	0.000057	0.000004	0.000000
0.000001	0.000057	0.002028	0.012251	0.002028	0.000057	0.000001
0.000002	0.000159	0.012251	0.941752	0.012251	0.000159	0.000002
0.000001	0.000057	0.002028	0.012251	0.002028	0.000057	0.000001
0.000000	0.000004	0.000057	0.000159	0.000057	0.000004	0.000000
0.000000	0.000000	0.000001	0.000002	0.000001	0.000000	0.000000

THIS IS FILTER # 35

0.000000	0.000000	0.000001	0.000001	0.000001	0.000000	0.000000
0.000000	0.000003	0.000043	0.000123	0.000043	0.000003	0.000000
0.000001	0.000043	0.001697	0.010824	0.001697	0.000043	0.000001
0.000001	0.000123	0.010824	0.949055	0.010824	0.000123	0.000001
0.000001	0.000043	0.001697	0.010824	0.001697	0.000043	0.000001
0.000000	0.000003	0.000043	0.000123	0.000043	0.000003	0.000000
0.000000	0.000000	0.000001	0.000001	0.000001	0.000000	0.000000

THIS IS FILTER # 36

0.000000	0.000000	0.000000	0.000001	0.000000	0.000000	0.000000
0.000000	0.000002	0.000032	0.000096	0.000032	0.000002	0.000000
0.000000	0.000032	0.001418	0.009554	0.001418	0.000032	0.000000
0.000001	0.000096	0.009554	0.955457	0.009554	0.000096	0.000001
0.000000	0.000032	0.001418	0.009554	0.001418	0.000032	0.000000
0.000000	0.000002	0.000032	0.000096	0.000032	0.000002	0.000000
0.000000	0.000000	0.000000	0.000001	0.000000	0.000000	0.000000

THIS IS FILTER # 37

0.000000	0.000000	0.000000	0.000001	0.000000	0.000000	0.000000
0.000000	0.000001	0.000024	0.000074	0.000024	0.000001	0.000000
0.000000	0.000024	0.001184	0.008425	0.001184	0.000024	0.000000
0.000001	0.000074	0.008425	0.961063	0.008425	0.000074	0.000001
0.000000	0.000024	0.001184	0.008425	0.001184	0.000024	0.000000
0.000000	0.000001	0.000024	0.000074	0.000024	0.000001	0.000000
0.000000	0.000000	0.000000	0.000001	0.000000	0.000000	0.000000

THIS IS FILTER # 38

0.000000	0.000000	0.000000	0.000000	0.000000	0.000000	0.000000
0.000000	0.000001	0.000018	0.000057	0.000018	0.000001	0.000000
0.000000	0.000018	0.000988	0.007424	0.000988	0.000018	0.000000
0.000000	0.000057	0.007424	0.965971	0.007424	0.000057	0.000000
0.000000	0.000018	0.000988	0.007424	0.000988	0.000018	0.000000
0.000000	0.000001	0.000018	0.000057	0.000018	0.000001	0.000000
0.000000	0.000000	0.000000	0.000000	0.000000	0.000000	0.000000

32	103	0.0016
33	83	0.0013
34	59	0.0009
35	50	0.0008
36	36	0.0006
37	25	0.0004
38	33	0.0005
39	13	0.0002
40	68	0.0011